



*m*THPP monoacetic ester: unexpected formation, zinc metalation, thermal and photophysical properties

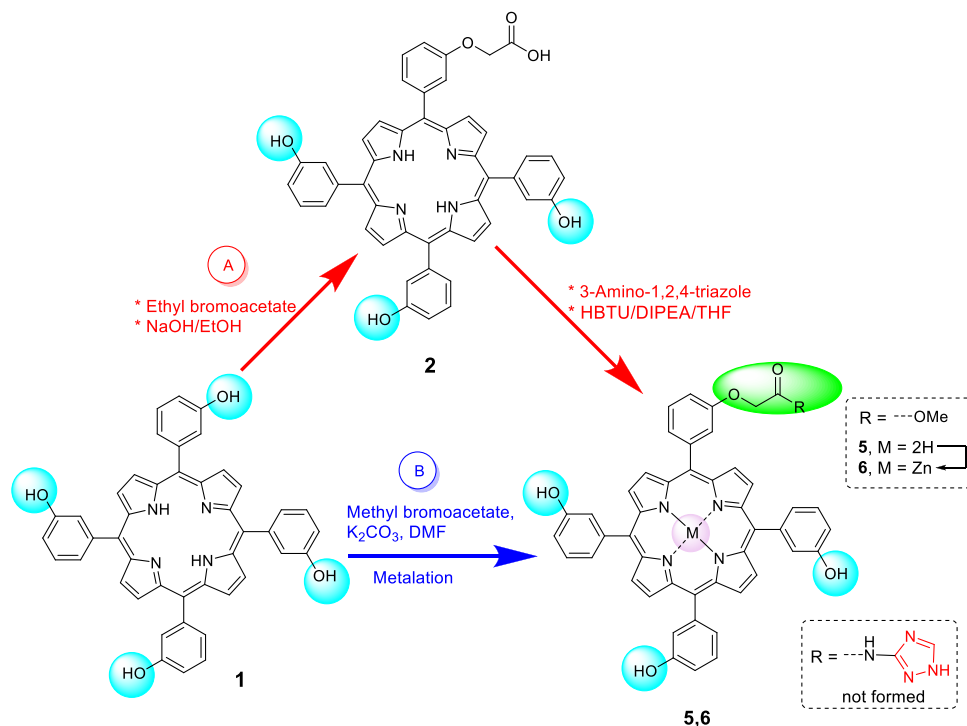
Ayman M. K. Sweed¹ · Yasser M. Shaker¹ · Sherif S. Ragab²

Received: 3 October 2022 / Accepted: 24 February 2023 / Published online: 16 March 2023
© The Author(s) 2023

Abstract

In the current investigation we report an unexpected methyl esterification occurred during the coupling reaction of *m*THPP monoacetic acid **2** with 3-amino-1,2,4-triazole in the presence of HBTU/DIPEA. The mechanism of this unexpected methyl esterification was studied, and the structure of the formed methyl ester **5** was confirmed by the means of ¹H, ¹³C NMR in addition to (MALDI-TOF and ESI-HRMS) spectrometry. The formation of **5** during the coupling reaction was also chemically supported by an alternative synthetic method involving a direct monosubstitution reaction of *m*THPP **1** with methyl bromoacetate. We also investigated the metalation of **5** with zinc and studied the thermal properties along with differential scanning calorimetry (DSC) of the zinc porphyrin **6**. The photophysical properties of porphyrin methyl ester **5** and its zinc complex **6** were also investigated.

Graphical Abstract



Keywords Synthesis · Esterification · *m*THPP-monoacid · Zinc metalloporphyrin · Thermogravimetric

Introduction

Porphyrins and their metallocomplexes are natural fascinating macrocycles of immense biological importance [1–3]. The usages of these molecules are not limited to photosensitization in photodynamic therapy. In fact, the diversity of the physicochemical properties of these fascinating molecules advocates them to be included in many technical applications such as catalysts, photocatalysts, optical monomers, sensors, solar cells and supramolecular chemistry [4–7].

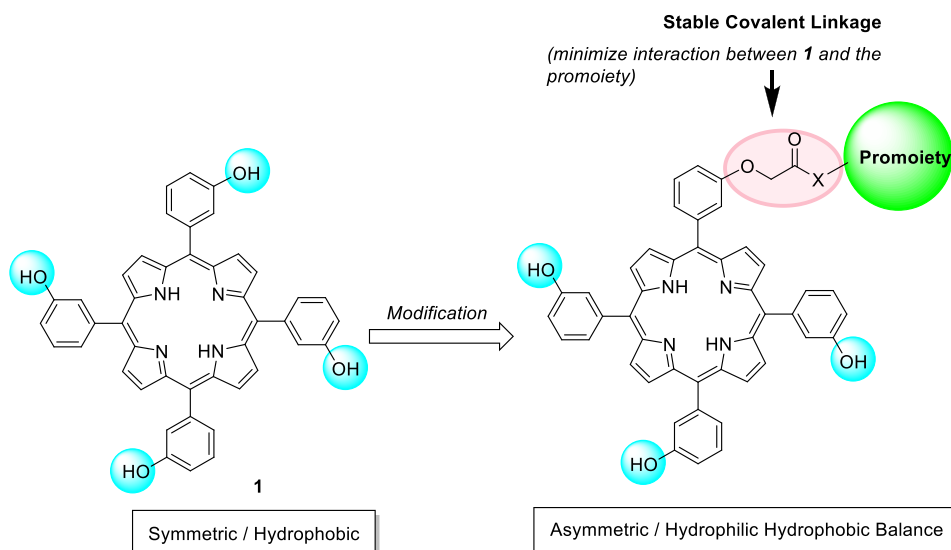
5,10,15,20-Tetrakis(*m*-hydroxyphenyl)porphyrin (*m*THPP, **1**) is a parent analog of the clinically approved drug Temoporfin® (*m*THPC) and was exploited in various PDT-related studies [8]. *M*THPP fulfills the ideal characteristics of photosensitizers, and it has enhanced physicochemical properties and high molar absorption coefficient at the red region [9]. *M*THPP could be easily accessible on large scale, and its periphery could be subjected to modification by biomolecules to improve both the pharmacological and physicochemical properties.

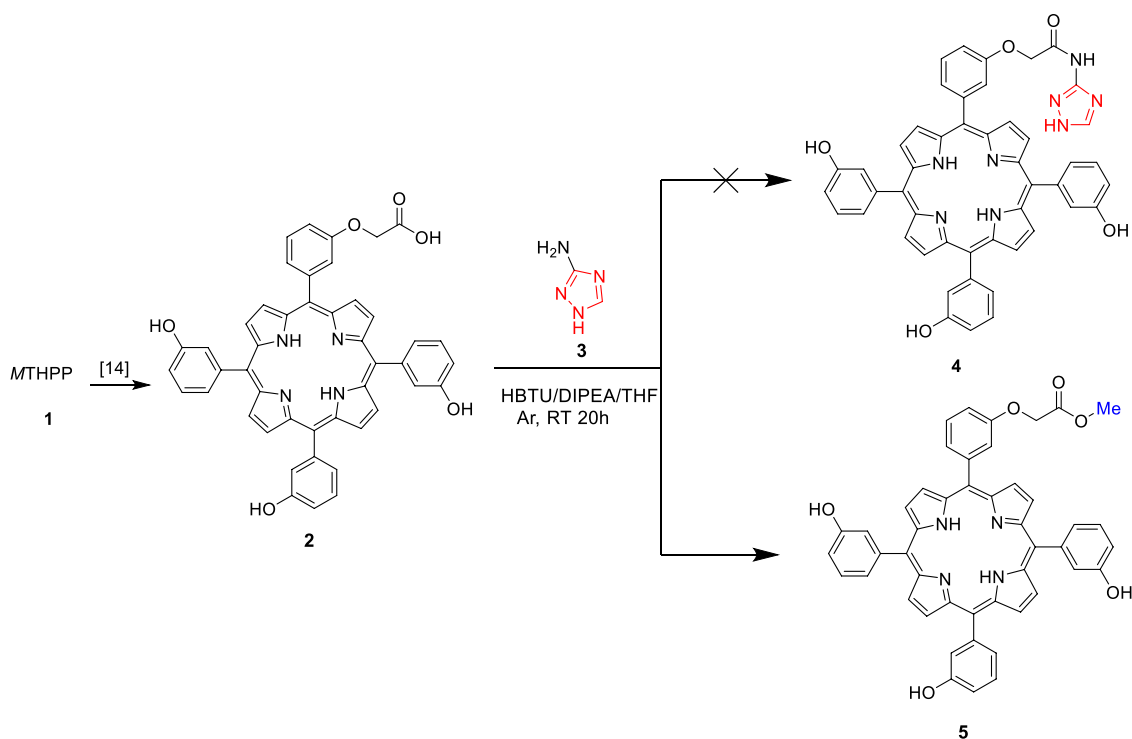
Regulation of the substituents at the *meso* position of *m*THPP can enhance its efficiency for PDT applications [1, 2]. Specifically, the carboxylic acid functionality has been extensively used in chemistry to build heterocycles and biological units onto the main building blocks for different applications [10, 11]. Additionally, the presence of both hydroxyl and carbonyl group in the same molecule can exhibit intramolecular hydrogen bonding leading to the stabilization of these compounds [12]. Introduction of one carboxylic acid group into *m*THPP could open the gate for the construction of asymmetric porphyrin derivatives

of the type A₃B [13, 14] which could be coupled to different molecules to get conjugates of interesting applications.

On the other hand, metalloporphyrin is considered the keystone in natural systems because most biochemical, photochemical, enzymatic functions depend on the distorted form of these macrocycles. It was reported that ligand-Zn(II) metal complexes showcased plausible potentials for antimicrobial and anticancer activities [15, 16]. Indeed, incorporation of a metal atom within porphyrins core allows further modification of the macrocycle for improved properties and applications [17]. One of the most interesting modification resulted from the insertion of metal ions with small ionic radius is the deviation from planarity compared to the porphyrin macrocycle [18]. Such distortion in metalloporphyrin macrocycle provides modified optical, electrochemical properties [19, 20]. Furthermore, metalation of porphyrin macrocycle plays an important role in improving the stability [21] as well as allowing promising catalytic activities for various metalloporphyrin macrocycles [22]. Pereira group reported an interesting review highlighted the most important examples for the utilization of *meso*-tetrasubstituted aryl metalloporphyrins as bioinspired oxidation catalysts [23]. Most of the research works in porphyrin and metalloporphyrin chemistry (either in our group or other research groups) depends on the synthetic chemistry approaches and diversity of applications. However, most of these approaches and applications are restricted by thermal properties of the synthesized porphyrin compounds. Surprisingly, there are a little thermal and thermochemical data for *m*THPP conjugates with stable covalent linkers and their metal complexes. Therefore, the study of the thermal behavior and thermal decomposition kinetics of this class of *meso*-tetrasubstituted porphyrin conjugates is of high interest.

Fig. 1 Modification of *m*THPP **1** for the design of new photosensitizers





Scheme 1 Unexpected methyl esterification of *m*THPP-monoacetic acid **2**

In a recent work, we reported a novel series of *m*THPP conjugates (Fig. 1) in which the *m*THPP-monoacetic acid was attached to bioactive heterocycles [14]. On application of the same reaction with triazole, unexpected methyl ester was formed instead of the porphyrin-triazole conjugate. In the current investigation we aim at discussing the unexpected methyl esterification of porphyrin monoacetic acid through suggesting two-path mechanism for formation of the unexpected adduct and chemically support its structure by an alternative synthetic method. We also aimed at investigating the zinc metalation of the unexpected product and studied the thermal properties of the formed zinc metalloporphyrin.

Results and discussion

In our recent study, we reported an efficient protocol to link *meso*-substituted porphyrin (*m*THPP) having one carboxylic group in one periphery **2** to heterocyclic nitrogen scaffolds via oxyacetamide linkage to enhance the targeting as well as the accumulation in cancer cells with tunable photophysical properties (Fig. 1) [14]. In fact, the conversion of *m*THPP **1** to its corresponding monoacetic acid derivative **2** is a suitable option which is commonly used for the synthesis of asymmetric porphyrin conjugates.

In order to achieve the conjugation of *m*THPP-monoacetic acid **2** with nitrogen heterocycles, we utilized the

standard coupling methodology. Specifically, uronium hexafluoro-phosphate (HBTU) was used as an efficient coupling agent to activate the -COOH functionality of *m*THPP-monoacetic acid **2** under mild basic conditions with the aid of *N,N*-diisopropylethylamine (DIPEA). Then, equimolar amounts of the amines were added for the formation of the porphyrin-heterocycles conjugates through oxyacetamide linker as depicted in Fig. 1. With this technique, we could access asymmetrical porphyrin derivatives of the type A_3B to add them as new photosensitizers to the porphyrin library.

We tried to apply the same coupling conditions to explore the reactivity of *m*THPP-monoacetic acid **2** toward different amino heterocycles such as 3-amino-1,2,4-triazole **3**. Surprisingly, the product displayed another unexpected direction under the above coupling condition, where the spectral analysis of the product obtained from the coupling reaction with the triazole **3** revealed that a methylation of the carboxylic acid periphery occurred rather than the expected coupling reaction. Thus, the unexpected *m*THPP methyl acetate **5** was formed instead of the porphyrin-triazole conjugate **4** (Scheme 1).

The structural assignment of porphyrin methyl ester **5** was supported by the means of ^1H , ^{13}C -NMR, and the mass spectrometry (MALDI-TOF and ESI-HRMS). Specifically, the ^1H -NMR of the product (Fig. 2a) showed the typical corresponding signals of *m*THPP (a singlet for the three hydroxyl protons (OH) at 9.89 ppm, a singlet for the eight β -protons

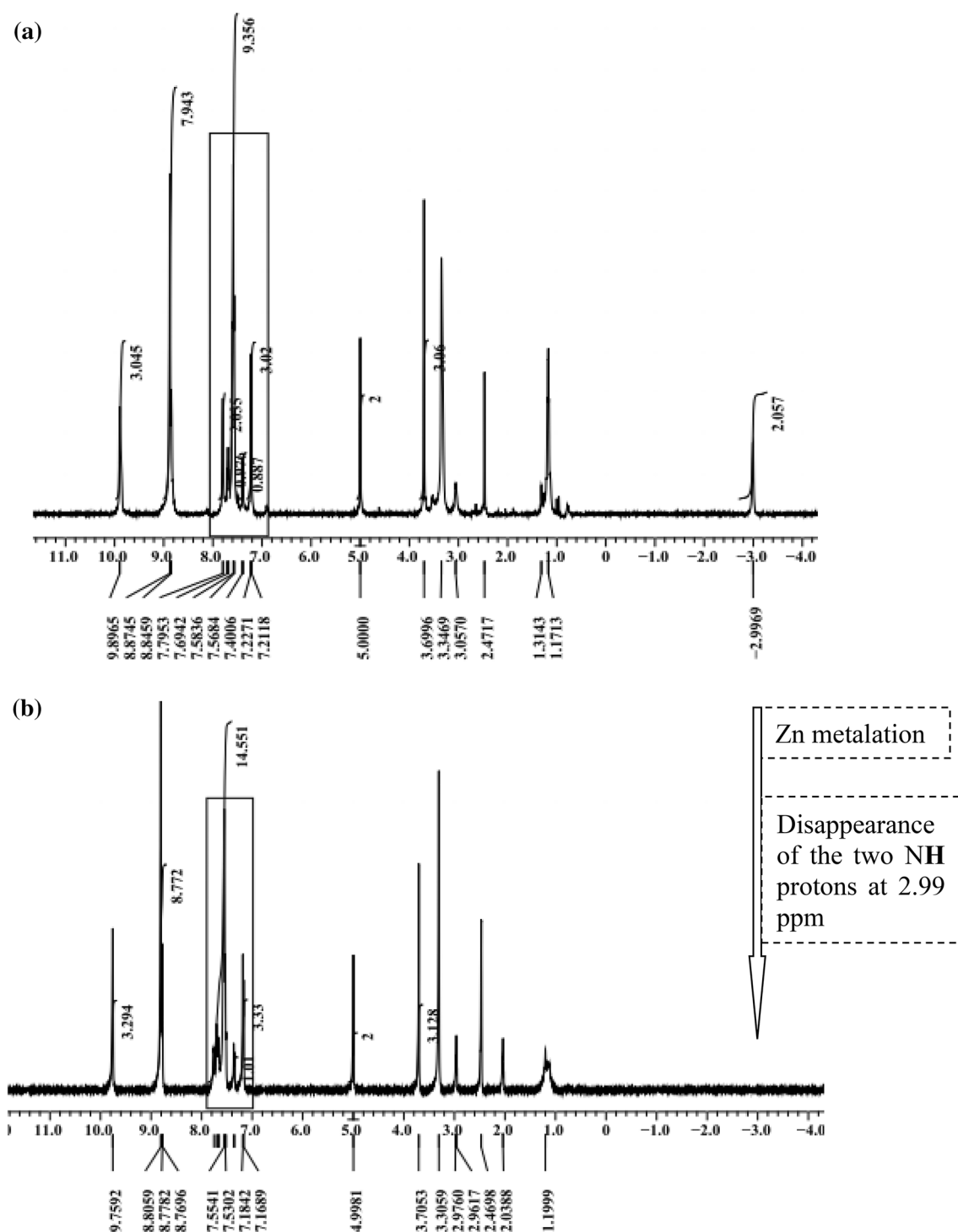


Fig. 2 $^1\text{H-NMR}$ spectra of compound **5** (a) and zinc porphyrin **6** (b)

at 8.87 ppm, the aromatic protons of the four phenyl rings at 7.21–7.79 ppm, and a singlet of the imine protons (2NH) at -2.99 ppm). Moreover, a singlet for the two methylene protons (OCH_2) appeared at 5.00 ppm. The most important distinguishable signal is a sharp singlet clearly appeared at 3.69 ppm corresponding to the methyl protons of the ester

group ($-\text{COOCH}_3$). The $^{13}\text{C-NMR}$ revealed the existence of the characteristic signal of methyl carbon ($-\text{COOCH}_3$) at 52.4 ppm, and the carbonyl carbon ($-\text{COOCH}_3$) was appeared at 169.8 ppm.

Additionally, the mass analysis (Fig. 3a and b) supported the assigned structure of **5**, where the MALDI-TOF-negative

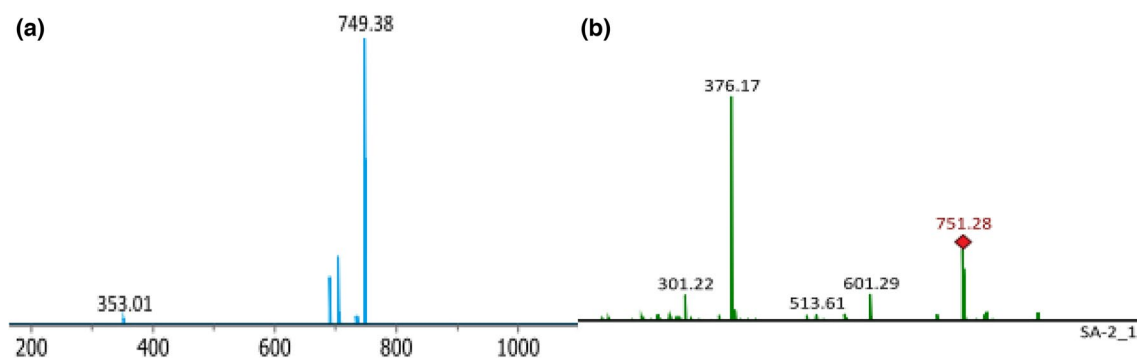


Fig. 3 MALDI-TOF-negative mode (a) positive mode (b) for compound **5**

and positive modes showed m/z at 749.38, 751.28, respectively. Moreover, the ESI-high-resolution mass spectrum of compound **5** showed m/z at 751.2565 corresponds to $C_{47}H_{34}N_4O_6$ ($M^+ + H$) (Fig. 4). From all these spectral data, the structural assignment of *m*THPP-monoacetic acid ester **5** confirmed the methyl ester esterification, while the structure **4** is ruled out.

In fact, the unexpected methylation of porphyrin is not rare, where Callot group reported that under the conditions of Eschenmoser's reaction a methylation of desoxyphylloerythroaetioporphylin (DPEP) was occurred and they suspected that methylene chloride (CH_2Cl_2) is the origin of the additional carbon [24]. In our case we did not use the methylene chloride or any of its analogs. Thus, we suspected that our coupling reagent may be responsible for the unexpected esterification. In this context, it was reported that tetramethylurea (TMU) is generated as a byproduct from the amide coupling reaction when HBTU used as coupling agent [25]. From the literature, we found that HBTU is not very stable under basic conditions and in the presence of moisture traces, HBTU undergoes a degradation leading to the formation of tetramethylurea (TMU) [26]. The latter reagent (TMU) could be exploited by Dep and Baruah as a methylene source for the first time [27].

To account for the unexpected methyl esterification, two paths are suggested as depicted in Scheme 2. The first path involves the classical activation of the monoacetic acid **2** with HBTU to form the activated acid (**I**) which preferred to react with TMU forming the methyl ester **5** rather than the conjugation with the amino-triazole. In the second path, TMU was directly generated in the first step from HBTU and reacted with the monoacetic acid **2** under the basic conditions affording the monoacetic acid ester **5**.

The formation of **5** during the coupling reaction was chemically supported by alternative method for preparation (Scheme 3). Where direct substitution on one of the hydroxyl group of *m*THPP **1** was achieved using methyl bromoacetate to afford a substitution product with identical physical, chemical, and spectroscopic data to those of the coupling reaction product **5**.

To improve the stability as well as allowing promising catalytic activities of *m*THPP-monoacetic acid ester **5**, we investigated its metalation through a smooth route using zinc diacetate at room temperature that quantitatively delivered zinc porphyrin **6** (Scheme 4). The 1H -NMR of zinc porphyrin **6** (Fig. 2b) showed the same signals as of *m*THPP-monoacetic acid ester **5** except for the corresponding singlet of the imine protons (2NH) at -2.99 ppm which was

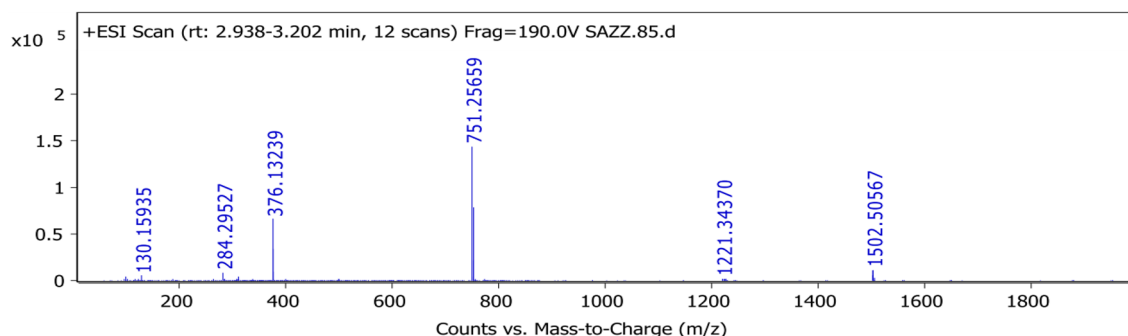
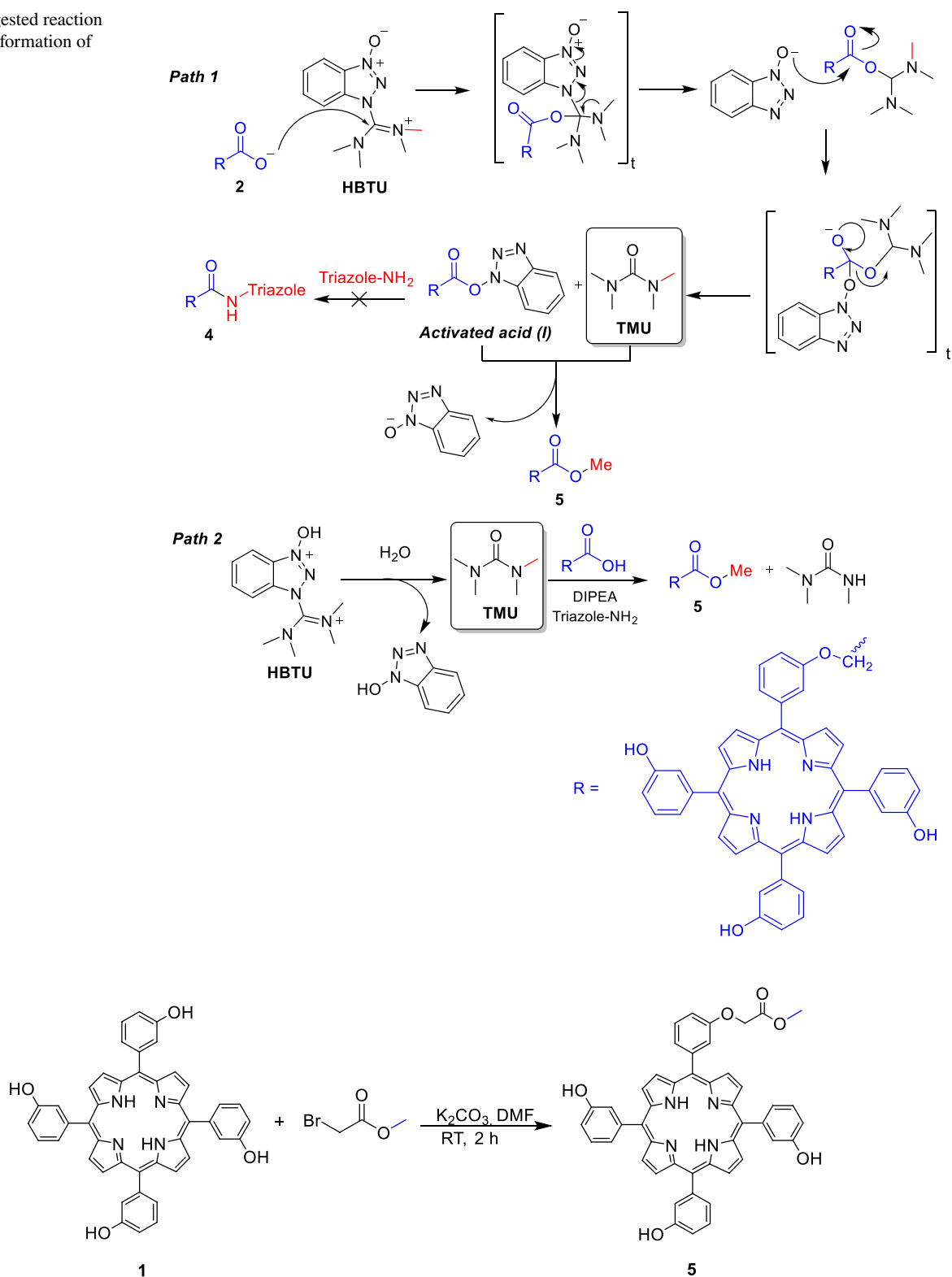
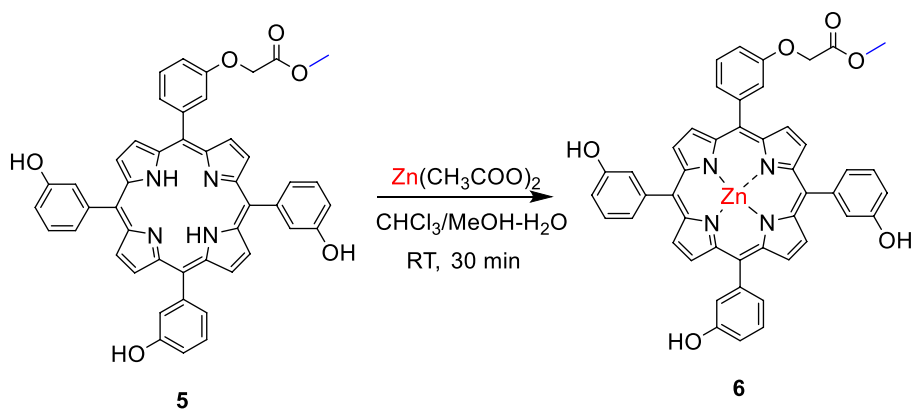


Fig. 4 ESI-HRMS spectrum of compound **5**

Scheme 2 Suggested reaction pathway for the formation of methyl ester **5**

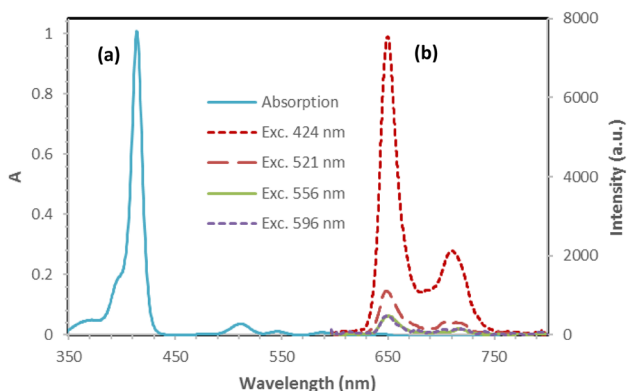


Scheme 3 Alternative method for the synthesis of **5**

Scheme 4 Zinc metalation of *m*THPP-monoacetic acid ester **5****Table 1** Photophysical properties of *m*THPP-ester **5** and zinc porphyrin **6**

Compound	Concentration (M)	Absorbance (λ_{\max}) (nm)	λ_{Em} (nm)	Molar extinction coefficient ϵ ($l\ mol^{-1}\ cm^{-1}$)
5	1.4×10^{-6}	1.009 (414), 0.03 (511), 0.01 (546), 0.007 (587), 0.003 (644)	650, 710	720,714 (414 nm), 26,535 (511 nm), 8071 (545 nm), 5700 (587 nm), 2371 (644 nm)
6	3.17×10^{-6}	0.91 (420), 0.05 (548)	595, 644	420 (274,169), 548 (1579)

Em = Emission, λ_{\max} = maximum wavelength

**Fig. 5** Absorption **a** emission spectra at different excitation wavelengths **b** of **5** (1.4×10^{-6} M, MeOH)

disappeared in the spectrum of **6**, confirming the realization of metalation.

Photophysical properties

The absorption and emission maxima as well as the molar absorption coefficient (ϵ) of *m*THPP-ester **5** and its zinc complex **6** are summarized in Table 1. The absorption and emission spectra showed the typical characteristics of *etio*-porphyrins as evidenced from Fig. 5. Specifically, the absorption spectrum (Fig. 5a) of *m*THPP-ester **5** in MeOH exhibited the corresponding intense Soret band at 414 nm and is typically as that of the porphyrin chromophore, while

the Q bands appeared broadened and red-shifted at 511, 545, 587, 644 nm. Moreover, the emission spectrum (Fig. 5b) of *m*THPP-ester **5** exhibited high fluorescence at 650, 710 nm, while the absorption spectrum (Fig. 6a) of zinc complex **6** showed the intense Soret band at 420 nm with a slight red shift, and just one Q band was clearly appeared at 548 nm. The corresponding fluorescence of zinc complex **6** was appeared in the emission spectrum as blue shifted bands at 595, 644 nm (Fig. 6b).

Thermal stability of zinc porphyrin **6**

The thermal gravimetric analysis (TGA) and differential scanning calorimetry (DSC) of zinc-porphyrin **6** were investigated to study the thermal properties upon metalation. From the TG curve (Fig. 7), we can conclude that there is no mass loss detected in the range of temperature from 25 to 243 °C. Over this temperature (243 °C), the decomposition of **6** starts involving successive three stages. The first stage (from 244 to 385 °C) involves a weight loss of 7.26% attributed to the removal of methyl carboxylate group (COOMe). During the second stage (from 386 to 516 °C) the mass had been lost with a percentage of 5.32% due to the removal of OCH₂ and one of the hydroxyl groups, while the last stage (from 516 to 900 °C) revealed a mass loss of 5.94% attributed to the removal of the last two hydroxyl groups. Interestingly, after 700 °C the residual mass percentage reached up 81.8%.

Fig. 6 Absorption **a** emission spectra **b** of **6** (3.17×10^{-6} M, CH_2Cl_2)

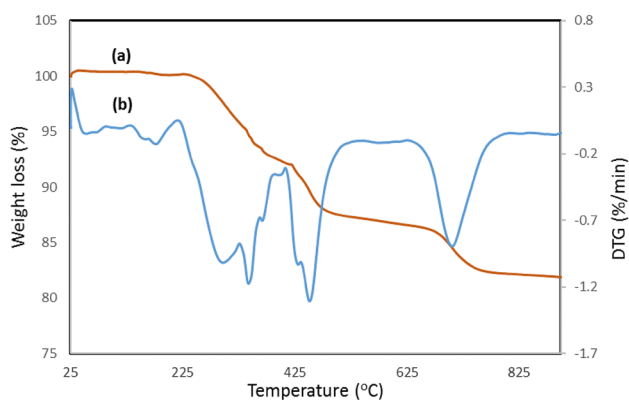
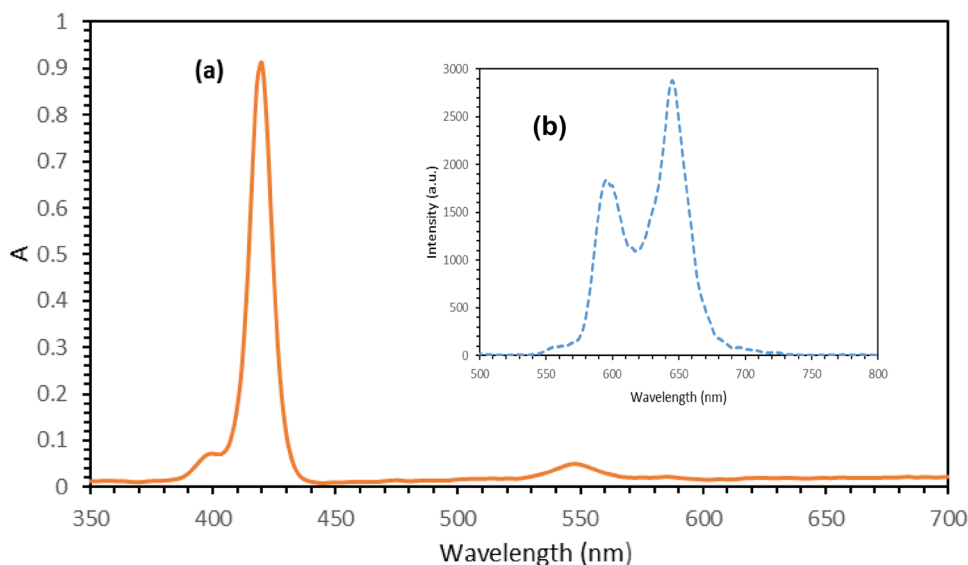


Fig. 7 TG curve **a** and DTG curve **b** of zinc metalloporphyrin **6**

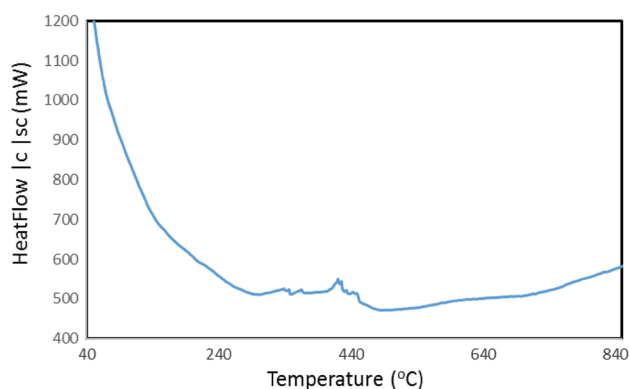


Fig. 8 DSC curve of zinc metalloporphyrin **6**

Simultaneously, the DSC curve (Fig. 8) showed two small exothermic peaks at 420 °C and 448 °C with T_{onset} values of 415 °C and 438 °C, respectively, corresponding to the

complete weight loss of $-\text{OCH}_2\text{COOMe}$ periphery and one hydroxyl groups. These obtained results confirm that the zinc metalloporphyrin **6** is thermally stable up to 243 °C, and the incorporation of a transition metal such as zinc into the ring system of porphyrins improves their thermal stability.

Experimental

Commercial and fine chemicals were purchased from Fisher Scientific, Sigma-Aldrich, and Acros Organics. THF was distilled over Na and kept dry over MS (4 Å). *MTHPP*-monoacetic acid **2** was synthesized following a procedure [14]. ^1H and ^{13}C NMR spectra of porphyrin materials were recorded on a JOEL ECA-500 spectrometer, ^1H NMR (500 MHz), ^{13}C NMR (125 MHz). The HRMS of porphyrin **5** was performed on a Q-TOF spectroscopy analysis at Faculty of Pharmacy-Fayoum University. UV-Vis absorption & emission spectra were recorded at Faculty of Science-Ain shams University using a Shimadzu MultiSpec-150 spectrophotometer. Thermal studies (TGA, DTG, DSC) were performed using a TGA-50H (Shimadzu) instrument at National Research Centre, Egypt, under N_2 atmosphere (heating rate is 10 °C/min), from 25 to 900 °C.

Synthetic procedure for methyl 2-(3-(10,15,20-tris(3-hydroxyphenyl)-porphyrin-5-yl)phenoxy)-acetate (**5**)

Method A

Under argon conditions, HBTU (0.165 mmol, 1.1 eq.) and DIPEA (0.45 mmol, 3 eq.) were added to a solution of

*m*THPP-acid **2** (0.15 mmol, 1 eq.) in 10 ml of dry THF. After stirring for 30 min. at r.t., 3-amino-1,2,4-triazole (0.225 mmol, 1.5 eq) was added and the reaction mixture was stirred for 20 h. After completion, H₂O was added to terminate the reaction, the organic phase was extracted by EtOAc, then washed with brine (3 × 20 mL) and H₂O (25 mL), and then dried over anhydrous Na₂SO₄, filtered, and the solvent was then removed under reduced pressure. The residue was purified by column chromatography (cc) using (CH₂Cl₂/MeOH, 90/0.5 to 90/2, v/v) to deliver the porphyrin ester **5** (70 mg, 65%) as purple powder.

Mp = 200–202 °C; *R*_f = 0.57 (CH₂Cl₂/MeOH, 5:0.1, v/v); ¹H-NMR ((CD₃)₂SO): δ_H = 9.89 (3H, s, OH), 8.87 (8H, s, β-H), 7.79 (2H, s, Ar-Hs), 7.69 (1H, t, *J*_{H,H} = 10 Hz, Ar-Hs), 7.57 (9H, t, *J*_{H,H} = 5 Hz, Ar-Hs), 7.40 (1H, d, *J*_{H,H} = 10 Hz, Ar-Hs), 7.22 (3H, d, *J*_{H,H} = 10 Hz, Ar-Hs), 5.00 (2H, s, OCH₂), 3.69 (3H, s, COOCH₃), -2.99 ppm (2H, s, NH). ¹³C-NMR ((CD₃)₂SO): δ_C = 169.9, 156.7, 156.3, 143.1, 142.9, 128.4, 126.4, 122.4, 121.3, 120.5, 119.9, 115.7, 115.1, 67.5, 52.4 ppm. (ESI-HRMS) *m/z* calcd for [C₄₇H₃₅N₄O₆] (M⁺ + H): 751.25566, found 751.2565; UV–Vis (MeOH): λ_{max} (log ε) = 414 (5.86), 511 (4.42), 546 (3.90), 587 (3.75), 644 (3.75).

Method B

5,10,5-Tris(3-hydroxyphenyl)-20-[(3-methyl acetoxy)phenyl]porphyrin (**5**)

A mixture of *m*THPP **1** (0.75 g, 1.1 mmol) and K₂CO₃ (0.15 g, 1.1 mmol) was dissolved in DMF (10 mL); then, methyl bromoacetate (0.12 ml, 1.1 mmol) was dropwise added. The reaction was allowed to stir at r.t. for 1.5 h. Once a decent amount of the monosubstituted porphyrin was formed (TLC monitored), DCM (50 mL) was added, then the organic layer was washed with brine (50 mL × 3), and water (50 mL × 3) then dried over anhydrous Na₂SO₄, and the solvent was removed with rotator evaporator. The crude material was purified with column chromatography by solvent system of CH₂Cl₂/hexane/MeOH (3:1:0.5 to 3:1:0.1, v/v/v) to yield **5** as a purple solid (150 mg, 20%).

Metalation of **5** (synthesis of {5,10,15-tris-(3-hydroxyphenyl)-20-[(3-methyl acetoxy)phenyl]porphyrinato}zinc(II) (**6**))

A solution of zinc diacetate (75 mg, 0.29 mmol, 3 eq) in MeOH/water was dropwise added to a stirred solution of **5** (70 mg, 0.095 mmol, 1 eq) in CHCl₃. After 30 min of stirring at r.t., the reaction mixture was diluted with CH₂Cl₂ and the organic layer was washed with water (30 mL × 3) and brine (30 mL × 3) and dried over anhydrous MgSO₄.

The solvent was removed under *vacuum* to afford zinc porphyrin complex **6** as bright purple solid (75 mg, 0.094 mmol, 98%).

Mp = 243–2245 °C; *R*_f = 0.34 (CH₂Cl₂/hexane/MeOH, 3: 2: 0.1, v/v/v); ¹H-NMR ((CD₃)₂SO): δ_H = 9.75 (3H, s, OH), 8.77 (8H, s, β-H), 7.75 (1H, s, Ar-Hs), 7.70 (1H, s, Ar-Hs), 7.66 (1H, t, *J*_{H,H} = 5 Hz, Ar-Hs), 7.58 (9H, m, Ar-Hs), 7.35 (1H, d, *J*_{H,H} = 10 Hz, Ar-Hs), 7.17 (3H, d, *J*_{H,H} = 10 Hz, Ar-Hs), 4.99 (2H, s, OCH₂), 3.70 ppm (3H, s, COOCH₃). UV–Vis (CH₂Cl₂): λ_{max} (log ε) = 420 (5.62), 548 (3.19).

Conclusions and outlook

In the current study, we discussed an unexpected methyl esterification occurred during the coupling reaction of *m*THPP monoacetic acid **2** with 3-amino-1,2,4-triazole in the presence of HBTU/DIPEA. We believed that tetramethylurea (TMU) which is generated from the coupling reagent (HBTU) is responsible for the unexpected esterification, and in this context, we suggested two-path mechanism for formation of the unexpected adduct.

The structure of the formed *m*THPP monoacetic ester **5** was confirmed by the means of spectrometry and also was chemically supported by alternative method for preparation involves the direct substitution on one of the hydroxyl group of *m*THPP **1** using methyl bromoacetate to afford the substitution adduct **5**. To improve the stability as well as allowing promising catalytic activities of *m*THPP-monoacetic acid ester **5**, we investigated its metalation through a smooth route using zinc diacetate at room temperature that quantitatively delivered zinc porphyrin. The thermal studies (including TGA, DTG, DSC) upon metalation were investigated, and their results confirm that the zinc metalloporphyrin **6** is thermally stable up to 243 °C, and the incorporation of a transition metal such as zinc into the ring system of porphyrins improves their thermal stability. The photophysical properties of porphyrin methyl ester **5** and its zinc complex **6** were also investigated, revealing a high value of the extinction coefficient. We anticipate that the current study could be beneficial to the porphyrin community by investigating the coupling reaction conditions and their effect on directing the reactions and also to shed more light on the thermal properties of porphyrins and their metalocomplexes and the potential of their usage in catalytic applications.

Acknowledgements This work was supported by the National Research Centre (NRC) through the internal project (No 12010112).

Funding Open access funding provided by The Science, Technology & Innovation Funding Authority (STDF) in cooperation with The Egyptian Knowledge Bank (EKB).

Declarations

Conflict of interest No competing financial interests to declare.

Open Access This article is licensed under a Creative Commons Attribution 4.0 International License, which permits use, sharing, adaptation, distribution and reproduction in any medium or format, as long as you give appropriate credit to the original author(s) and the source, provide a link to the Creative Commons licence, and indicate if changes were made. The images or other third party material in this article are included in the article's Creative Commons licence, unless indicated otherwise in a credit line to the material. If material is not included in the article's Creative Commons licence and your intended use is not permitted by statutory regulation or exceeds the permitted use, you will need to obtain permission directly from the copyright holder. To view a copy of this licence, visit <http://creativecommons.org/licenses/by/4.0/>.

References

- J.F. Algorri, M. Ochoa, P. Roldán-Varona, L. Rodríguez-Cobo, J.M. López-Higuera, *Cancers (Basel)* **13**(17), 4447 (2021)
- H. Mahmoudi, A. Bahador, M. Pourhajibagher, M.Y. Alikhani, *J. lasers med. sci.* **9**(3), 154 (2018)
- M. Imran, M. Ramzan, A.K. Qureshi, M.A. Khan, M. Tariq, *Bio-sens.* **8**(4), 95 (2018)
- C. Zhang, P. Chen, H. Dong, Y. Zhen, M. Liu, W. Hu, *Adv. Mater.* **27**(36), 5379–5387 (2015)
- G.D. Bajju, S. Kundan, M. Bhagat, D. Gupta, A. Kapahi, G. Devi, *Bioinorg. Chem. Appl.* **2014**, 782762 (2014). <https://doi.org/10.1155/2014/782762>
- M. Lv, X. Ren, R. Cao, Z. Chang, X. Chang, F. Bai, Y. Li, *Polymer* **14**(22), 4893 (2022)
- K. Anjali, L. Nishana, J. Christopher, A. Sakthivel, J. Porous Mater. **27**(4), 1191 (2020)
- M.O. Senge, J.C. Brandt, *Photochem. Photobiol.* **87**(6), 1240 (2011)
- M. Ethirajan, Y. Chen, P. Joshi, R.K. Pandey, *Chem. Soc. Rev.* **40**(1), 340–362 (2011)
- N. Malatesti, I. Munitic, I. Jurak, *Biophys. rev.* **9**(2), 149 (2017)
- N. Tsolekile, S. Nelana, O.S. Oluwafemi, *Molecules* **24**(14), 2669 (2019)
- G.-I. Badea, G.L. Radu, *Carboxylic acid: key role in life sciences IntechOpen*, 2018). <https://doi.org/10.5772/intechopen.77021>
- A.M. Sweed, M.O. Senge, S.M.S. Atta, D.S. Farrag, A.-R.H. Abdel-Rahman, Y.M. Shaker, *J. Porphyr Phthalocyanines* **22**(11), 997 (2018)
- A.M. Sweed, S.S. Ragab, Y.M. Shaker, *J. Porphyr Phthalocyanines* **26**(10), 648–655 (2022)
- M. Tarafder, K.T. Jin, K.A. Crouse, A. Ali, B. Yamin, H.-K. Fun, *Polyhedron* **21**(25–26), 2547 (2002)
- J. Sheikh, H. Juneja, V. Ingle, P. Ali, T.B. Hadda, *J. Saudi Chem. Soc.* **17**(3), 269 (2013)
- I. Beletskaya, V.S. Tyurin, A.Y. Tsivadze, R. Guilard, C. Stern, *Chem. Rev.* **109**(5), 1659 (2009)
- T. Ishizuka, N. Grover, C.J. Kingsbury, H. Kotani, M.O. Senge, T. Kojima, *Chem. Soc. Rev.* **51**(17), 7560 (2022). <https://doi.org/10.1039/D2CS00391K>
- M.O. Senge, *Chem. Comm.* **3**, 243 (2006)
- Y. Song, R.E. Haddad, S.-L. Jia, S. Hok, M.M. Olmstead, D.J. Nurco, N.E. Schore, J. Zhang, J.-G. Ma, K.M. Smith, *J. Am. Chem. Soc.* **127**, 1179–1192 (2005)
- X. Wei, X. Du, D. Chen, Z. Chen, *Thermochim. Acta* **440**, 181–187 (2006)
- P. Gotico, Z. Halime, A. Aukauloo, *Dalton Trans.* **49**, 2381 (2020)
- M.M. Pereira, L.D. Dias, M.J. Calvete, *Metalloporphyrins: bio-inspired oxidation catalysts. ACS Catal.* **8**, 10784 (2018)
- C. Jeandon, R. Ocampo, H.J. Callot, *Tetrahedron* **53**, 16107 (1997)
- Y. Yang, L. Hansen, J.K. Sjögren, I.R. León, J.-M. Receveur, F. Badalassi, *Org. Process Res. Dev.* **25**, 1923 (2021)
- F. Albericio, J.M. Bofill, A. El-Faham, S.A. Kates, *J. Org. Chem.* **63**, 9678 (1998)
- M.L. Deb, P.J. Borpatra, P.J. Saikia, P.K. Baruah, *Org. Biomole. Chem.* **15**, 1435 (2017)

Authors and Affiliations

Ayman M. K. Sweed¹ · Yasser M. Shaker¹ · Sherif S. Ragab² 

✉ Sherif S. Ragab
she2rifx@yahoo.com

¹ Department of the Chemistry of Natural and Microbial Products, Pharmaceutical and Drug Industries Research Institute, National Research Centre, El-Behouth St., Dokki, Cairo 12622, Egypt

² Photochemistry Department, Chemical Industries Research Institute, National Research Centre, El-Behouth St., Dokki, Cairo 12622, Egypt